

Structural investigation of Ca/Si(111) surfaces

Kazuyuki Sakamoto,^{1,2,*} Wakaba Takeyama,² H. M. Zhang,¹ and R. I. G. Uhrberg¹

¹*Department of Physics and Measurement Technology, Linköping University, S-581 83 Linköping, Sweden*

²*Department of Physics, Graduate School of Science, Tohoku University, Sendai, 980-8578, Japan*

(Received 18 March 2002; revised manuscript received 5 July 2002; published 29 October 2002)

The surface structures of different Ca/Si(111) surfaces were studied by low-energy electron diffraction (LEED) and high-resolution core-level photoelectron spectroscopy. Five different phases were observed in LEED depending on the Ca coverage. The lowest coverage phase has both (3×2) and $c(6 \times 2)$ periodicities, and the highest coverage phase has a (2×1) periodicity. The LEED patterns of the three intermediate phases were (5×2) , (7×1) , and (9×1) . In the Si $2p$ core-level spectra, three surface components were observed in both the lowest and highest coverage phases. These three surface components were also observed in each intermediate phase together with two other components. The presence of the two extra components indicates that the intermediate phases are not completely described by simple combinations of the two end phases as suggested in the literature. By considering the energy shift and intensity of each surface component, we conclude that the structure of the (3×2) phase is basically the same as that of the honeycomb-chain-channel model with a Ca coverage of $1/6$ ML, and the (2×1) phase is formed by π -bonded Seiwatz Si chains with a coverage of 0.5 ML. Moreover, taking the energy shifts and intensities of the extra surface components into account, we propose a structural model of the (5×2) phase, whose Ca coverage is 0.3 ML.

DOI: 10.1103/PhysRevB.66.165319

PACS number(s): 68.35.-p, 79.60.-i, 61.14.Hg

I. INTRODUCTION

Motivated by the fundamental and technological importance, one-dimensional (1D) structures formed on semiconductor surfaces is a topic of increasing interest. From a scientific point of view, a number of interesting phenomena has been reported for these 1D structures.^{1,2} The Si(111)- $(n \times 1)$ structures formed by the adsorption of alkaline-earth metals (AEM's) are candidates for such 1D systems.

The Ca/Si(111) surface is known to form a series of $(n \times 1)$ reconstructions ($n = 3, 5,$ and 7) that culminates with a (2×1) phase at 0.5 ML.^{3,4} The lowest coverage (3×1) phase is also formed by the adsorption of monovalent alkali metals (AM's) and Ag, and divalent rare-earth metals (Sm and Yb) with a coverage of $1/3$ ML. The similarity of the low-energy electron diffraction (LEED) I - V curves,^{5,6} scanning-tunneling-microscopy (STM) images,⁷⁻¹¹ and surface core-level shift (SCLS) measurements^{9,12-15} strongly suggests that all (3×1) surfaces have a quite similar structure. Among the large number of proposed structural models, the honeycomb-chain-channel (HCC) model,¹⁶⁻¹⁸ which is energetically more stable than the other models and fully compatible with the SCLS results and the STM images, is widely believed to be the most appropriate geometric structure of the Si(111)- (3×1) surface.

The electronic structures of the (3×1) surfaces formed by monovalent atom adsorption are expected to show semiconducting characters according to the even number of valence electrons in the unit cell. This expectation agrees well with the semiconducting electronic structures obtained experimentally.^{8,13,14,19,20} However, in the case of AEM adsorption, experimental studies reported semiconducting characters for Ca,³ Mg,²¹ and Ba (Ref. 22) adsorbed Si(111)- (3×1) surfaces though the electronic structures are anticipated to show metallic characters according to the electron counting. Regarding the Ba adsorbed surface, this inconsistency

was explained by the presence of a (3×2) periodicity, which was clearly observed using STM (Ref. 23) but not in electron diffraction studies,^{22,24} and by the Ba coverage.²³ That is, a surface with a (3×2) periodicity and a Ba coverage of $1/6$ ML lead to an even number of valence electrons in the unit cell, and thus explain well the semiconducting character of the so-called Ba/Si(111)- (3×1) surface. In contrast to the Ba case, the semiconducting characters of Ca (Ref. 3) and Mg (Ref. 21) adsorbed Si(111)- (3×1) surfaces were proposed to result from a Mott or a CDW transition that might occur due to strong electron correlations which can originate from the 1D structure. The propositions for the origins of the transitions were based on the assumption that the geometric structures of these surfaces are completely the same as the HCC model, i.e., a surface with a (3×1) periodicity and an adsorbate coverage of $1/3$ ML. However, so far there is no detailed study about the geometric structure of the Ca/Si(111)- (3×1) surface, and thus there is no evidence to support these propositions.

Concerning the other Ca/Si(111) phases, the (2×1) phase was proposed to be formed by π -bonded Seiwatz Si chains, and the two intermediate phases [the (5×1) and (7×1) phases] were proposed to be formed by simple combinations of the HCC model and the Seiwatz model.^{3,4} The electronic structures of these (5×1) , (7×1) , and (2×1) phases were reported to show semiconducting characters.³ Among these three phases, the semiconducting electronic structure of the (2×1) phase agrees well with the even number of valence electrons in the unit cell, whereas those of the two intermediate phases are inconsistent with the electronic character expected by electron counting. In similarity with the (3×1) phase, the origins of the semiconducting electronic structures of the two intermediate phases are not determined so far. Further, there is no experimental evidence that supports the proposition about the geometric structures of the intermediate phases.

In this paper, we present detailed coverage-dependent LEED and high-resolution Si $2p$ core-level studies of the Ca/Si(111) surfaces. In the LEED study, five different phases were observed at different Ca coverages. The lowest coverage phase has both (3×2) and $c(6 \times 2)$ periodicities, the highest coverage phase has a (2×1) periodicity, and the three intermediate phases have (5×2) , (7×1) , and (9×1) periodicities. In the Si $2p$ core-level spectra, three surface components were observed in both the lowest and highest coverage phases. Taking the energy shift and intensity of each surface component into account, we conclude that the (3×2) and (2×1) phases have the HCC structure with a Ca coverage of $1/6$ ML and the Seiwatz structure with a coverage of 0.5 ML, respectively. A (3×2) periodicity with a Ca coverage of $1/6$ ML leads to an even number of valence electrons, and thus explains well the semiconducting electronic structure of the so-called Ca/Si(111)- (3×1) surface. Together with the three surface components observed in the lowest and highest coverage phases, two other components were observed in the three intermediate phases. The presence of extra surface components indicates that the intermediate phases are not formed by simple combinations of the two end phases. By considering the energy shifts and intensities of the extra surface components, we propose a structural model for the (5×2) phase whose Ca coverage is 0.3 ML. The (5×2) unit cell and the 0.3 ML Ca coverage elucidate the semiconducting character of this phase.

II. EXPERIMENTAL DETAILS

The high-resolution photoemission measurements and LEED studies were performed at beamline 33 at the MAX-I synchrotron radiation facility in Lund, Sweden. The Si $2p$ core-level spectra were obtained with an angle-resolved photoelectron spectrometer with a total-energy resolution of ~ 80 meV and an angular resolution of $\pm 2^\circ$. The Si(111) sample, cut from a Sb-doped (n -type, $3 \Omega\text{cm}$) Si wafer, was preoxidized chemically before it was inserted into the vacuum system. To obtain a clean surface, we annealed the sample at 1230 K by direct resistive heating in the vacuum chamber to remove the oxide layer, and at 1520 K to remove carbon contamination from the surface. After the annealing, we observed a sharp (7×7) LEED pattern, and neither the valence-band spectra nor the Si $2p$ core-level spectra showed any indication of contamination. Each Ca/Si(111)- $(n \times 1)$ reconstruction was prepared by either depositing a certain amount of Ca onto the clean Si(111)- (7×7) surface that was subsequently annealed at approximately 825 K, or by reducing the Ca coverage by annealing the 0.5 ML Ca adsorbed Si(111)- (2×1) surface at a temperature between 900 and 1050 K. All LEED and core-level studies were performed after cooling the sample down to 100 K.

III. RESULTS

A. LEED

Figures 1(a)–(e) show the LEED patterns of the Ca/Si(111) phases formed at different coverages. The LEED pat-

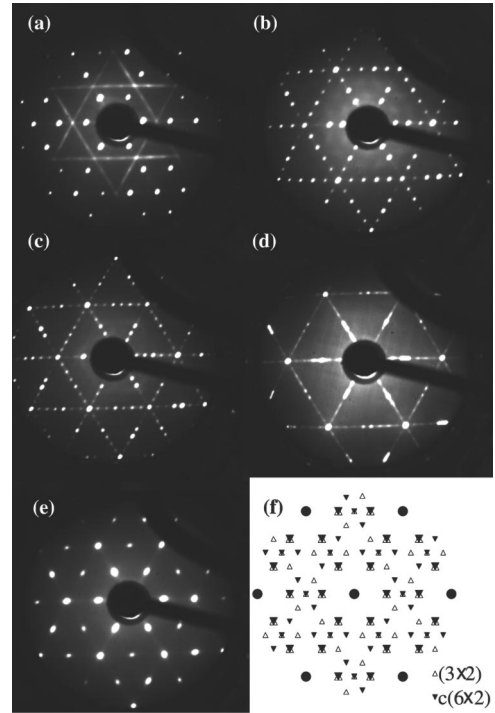


FIG. 1. LEED patterns of the Ca/Si(111) surfaces obtained at different coverages. Ca coverage increases in the order of (a) \rightarrow (b) \rightarrow (c) \rightarrow (d) \rightarrow (e). Primary electron energies are (a) 52 eV, (b) 67 eV, (c) 70 eV, (d) 52 eV, and (e) 76 eV. All patterns are obtained after cooling the sample down to 100 K. (f) shows the schematic LEED patterns of a three domains Si(111)- (3×2) surface and a three domains Si(111)- $c(6 \times 2)$ surface.

tern of the lowest coverage phase is displayed in Fig. 1(a), and the Ca coverage increases in the order of (a) \rightarrow (b) \rightarrow (c) \rightarrow (d) \rightarrow (e). Together with the $\times 3$ spots, some extra spots are clearly observed in Fig. 1(a). Comparing the LEED pattern shown in Fig. 1(a) with the schematic LEED patterns of Si(111)- (3×2) and $-c(6 \times 2)$ surfaces [Fig. 1(f)], we conclude that the lowest coverage phase consists of large (3×2) and $c(6 \times 2)$ domains. This result obtained at 100 K is different from the results obtained at room temperature using STM (Ref. 3, 4, 10) in which only local (3×2) and $c(6 \times 2)$ structures were observed. It is also different from the results of previous electron diffraction studies in which only weak $\times 2$ streaks were observed at room temperature,^{4,10} and no trace of $\times 2$ was observed at a higher temperature.³ Taking into account that the (3×2) structure was reported to be formed by 1D chains that show $\times 2$ modulation along each chain by STM,^{4,10} these thermal-dependent results suggest that the correlation between a $\times 2$ periodicity along a chain and the $\times 2$ periodicity along the neighboring chains becomes weaker at higher temperatures. That is, the basic structure of the lowest coverage Ca/Si(111) phase has (3×2) and $c(6 \times 2)$ periodicities, and the observation of only a (3×1) periodicity at high temperatures results from thermal-induced disorder of the $\times 2$ periodicity.

In Fig. 1(b), sharp $\times 5$ spots are observed together with dim diffuse spots. Since no trace of other phases [e.g., spots originating from a (3×2) phase] is observed in Fig. 1(b),

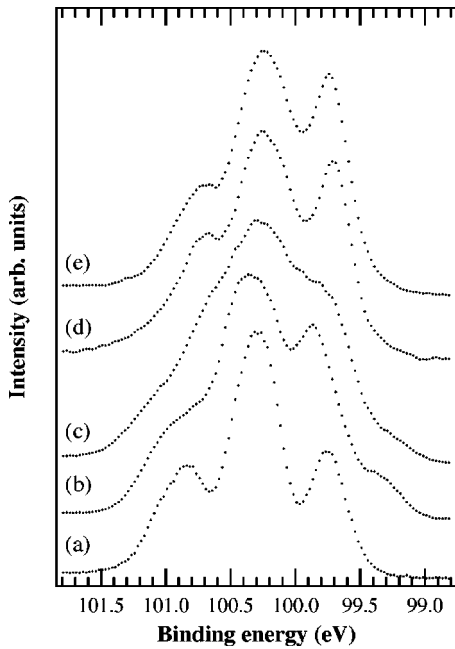


FIG. 2. Si $2p$ core-level spectra of the Ca/Si(111) surfaces measured at 100 K with $h\nu=135$ eV and $\theta_e=60^\circ$. (a) is the spectrum of the $(3\times'2')$ phase, (b) the $(5\times'2')$ phase, (c) the $(7\times'2')$ phase, (d) the $(9\times'2')$ phase, and (e) the $(2\times'1)$ phase. The spectra are obtained from the same surfaces as those used in Fig. 1.

these dim spots originate from the so-called Ca/Si(111)- $(5\times'1)$ surface itself. The positions of these dim spots correspond to the positions of the $\times 2$ spots of $(5\times'2)$ and $c(10\times'2)$ structures. Thus, the presence of these dim spots indicates that the basic structure of the so-called Ca/Si(111)- $(5\times'1)$ surface has actually both $(5\times'2)$ and $c(10\times'2)$ periodicities, and suggests that this surface is basically formed by combinations of the $(3\times'2)$ and $(2\times'1)$ phases. Below, we call the mixed Ca/Si(111)- $(3\times'2)$ and $c(6\times'2)$ surface as the Ca/Si(111)- $(3\times'2')$ surface, and the mixed Ca/Si(111)- $(5\times'2)$ and $c(10\times'2)$ surface as the Ca/Si(111)- $(5\times'2')$ surface to simplify the description. Figures 1(c) and 1(e) show the LEED pattern of the Ca/Si(111)- $(7\times'1)$ and $(2\times'1)$ surfaces, and Fig. 1(d) displays the pattern of the Ca/Si(111)- $(9\times'1)$ surface that was not reported in the previous studies.^{3,4,10} Taking the observation of the $(5\times'2')$ phase into account, the two other intermediate phases might also be basically formed by combinations of the $(3\times'2')$ and $(2\times'1)$ phases, and we propose that these two phases have actually $(7\times'2')$ and $(9\times'2')$ periodicities. The invisible $\times 2$ spots and/or $\times 2$ streaks of the $(7\times'2')$ and $(9\times'2')$ phases in Fig. 1 can be explained by the long distances between $\times 2$ chains that lead to very weak correlation between the neighboring $\times 2$ periodicity chains.

B. Si $2p$ core level

Figure 2 shows the Si $2p$ core level spectra of the five phases observed using LEED. The spectra were obtained from the same surfaces as those used in Fig. 1. A photon

energy ($h\nu$) of 135 eV and an emission angle (θ_e) of 60° from the surface normal direction were used for all spectra. The spectral shapes of the $(3\times'2')$ and $(2\times'1)$ phases are quite similar with those observed previously,³ whereas the shapes of the $(5\times'2')$ and $(7\times'2')$ phases are different. This difference might come from the different quality of the samples used in the previous study. For example, since the difference in Ca coverages of the $(5\times'2')$ and $(7\times'2')$ phases is small, i.e., less than 0.03 ML in the model proposed in the previous studies,^{3,4} and the sample was annealed at a temperature high enough to desorb Ca atoms to form those phases, an uneven heated sample might produce a difference in Ca coverage and thus different phases at different sample positions. In the present study, the high quality of each sample is confirmed by LEED.

In order to determine the number of Si $2p$ components that compose the spectra shown in Fig. 2, we have measured each phase using different $h\nu$ and θ_e that give a difference in the surface sensitivity. We have used $(h\nu, \theta_e)=(135$ eV, $60^\circ)$ for the most surface sensitive measurement, and $(h\nu, \theta_e)=(108$ eV, $0^\circ)$ for the most bulk sensitive measurement. In Fig. 3 we show the $h\nu$ - and θ_e -dependent Si $2p$ core-level spectra of the Ca/Si(111)- $(3\times'2')$, $(2\times'1)$, and $(5\times'2')$ surfaces. Without any processing, the spectra of the $(3\times'2')$ phase reveal the presence of several components that contribute to the shape of the spectra. The most evident one is $S1$, whose $2p_{3/2}$ component is clearly observed at a binding energy (E_B) of 99.75 eV. The presence of $S2$ is revealed by the behavior of the valley between the $2p_{3/2}$ components of $S1$ and B . That is, the flat part observed at around $E_B=99.9$ eV in the spectra obtained at $(h\nu, \theta_e)=(145$ eV, $0^\circ)$ is impossible to reproduce by using only $S1$. The contribution from a third component ($S3$) is confirmed by the observation of its $2p_{3/2}$ component as a shoulder at $E_B=100.4$ eV in the spectra measured at $(h\nu, \theta_e)=(135$ eV, $0^\circ)$, and by its $2p_{1/2}$ component that is observed as a shoulder at $E_B=101$ eV using $(h\nu, \theta_e)=(135$ eV, $60^\circ)$. The presence of three surface components is also revealed for the $(2\times'1)$ phase. $S1$ is clearly observed as a peak at $E_B=99.75$ eV, and the presence of $S2$ and $S3$ is recognized from the broadening of the $2p_{3/2}$ component of B in the spectra obtained with high surface sensitivity.

Taking its complicate spectral shape into account, one easily knows that the number of surface components of the $(5\times'2')$ phase is larger than those of the $(3\times'2')$ and $(2\times'1)$ phases. $S2$ is observed as a peak with $(h\nu, \theta_e)=(135$ eV, $60^\circ)$ at $E_B=99.9$ eV. $S1$ is revealed by the tail on the low binding energy side of the $2p_{3/2}$ component of $S2$. $S3$ is obvious from the observation of a shoulder in the spectrum obtained with $(h\nu, \theta_e)=(135$ eV, $0^\circ)$, and the observation of a clear peak at $(h\nu, \theta_e)=(135$ eV, $60^\circ)$. The presence of $S4$ is revealed by the peak observed at around 99.35 eV using $(h\nu, \theta_e)=(135$ eV, $60^\circ)$, and the small structure observed at the same E_B in other spectra. The contribution from a fifth component $S5$ is deduced by the long tail on the high binding energy side that extends to 101.4 eV in the spectrum obtained with $(h\nu, \theta_e)=(135$ eV, $60^\circ)$. The $h\nu$ - and θ_e -dependent Si $2p$ core-level spectra of the

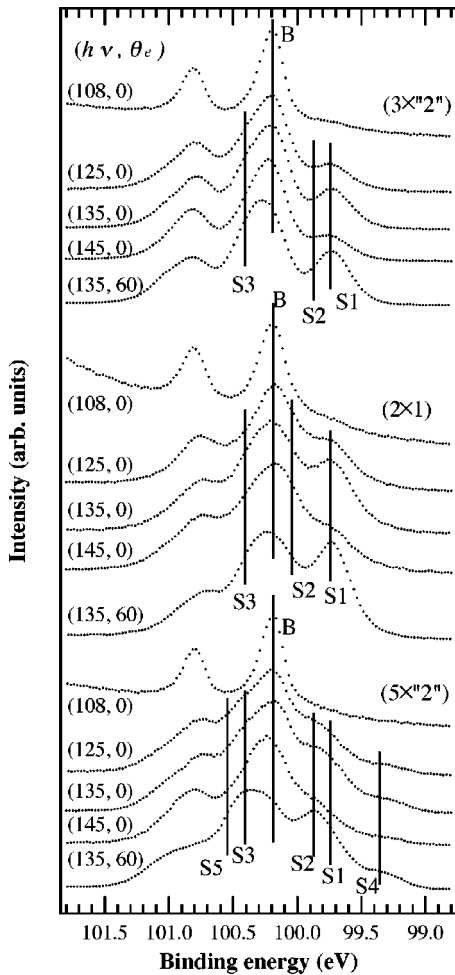


FIG. 3. Si $2p$ core-level spectra of the Ca/Si(111)-(3×2), (2×1), and (5×2) surfaces measured at different $h\nu$ and θ_e . The solid lines indicate the energy positions of the Si $2p_{3/2}$ parts of the four components for the (3×2) and (2×1) phases, and of the six components for the (5×2) phase.

(7×2) and (9×2) phases, which are not shown here, also reveal the presence of five surface components each in similarity with the (5×2) phase.

IV. DISCUSSION

Quantitative information about the structures of the Ca/Si(111) surfaces, is obtained by analyzing the Si $2p$ spectra by a standard least-squares-fitting method using spin-orbit split Voigt functions. Figure 4 shows the results of the analysis for the Si $2p$ core-level spectra of the Ca/Si(111) surfaces obtained with $(h\nu, \theta_e) = (135 \text{ eV}, 60^\circ)$. The open circles are the experimental data, and the solid lines overlapping the data are the fitting curves. We used 608 meV for the spin-orbit splitting and a 80 meV full width at half maximum (FWHM) for the Lorentzian contribution for all components in the fitting procedure. The Gaussian widths of the bulk components are 225 meV (FWHM) for all surfaces, and those of the surface components are between 268 and 312 meV. A polynomial background was subtracted before the

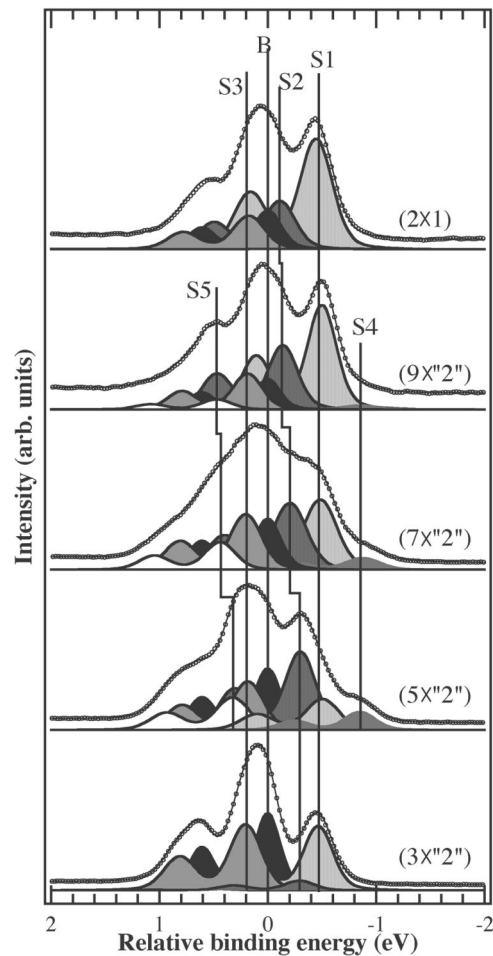


FIG. 4. Decomposition of the Si $2p$ core-level spectra of the Ca/Si(111)-(3×2), (5×2), (7×2), (9×2), and (2×1) surfaces. All spectra were recorded with $h\nu = 135 \text{ eV}$ and $\theta_e = 60^\circ$. The open circles are the experimental data, and the solid lines overlapping the open circles are the fitting curves. Each component is indicated by different hatching.

decomposition of each spectrum, and each component is indicated by different hatching.

From the result of the fitting procedure, we can conclude that both the (3×2) and (2×1) phases have three surface components, a number which is larger than that reported previously.³ We can also conclude that the three other phases have five surface components each. Among the surface components, S1 and S3 are observed in all phases at the same binding energy, and S2 is observed in all phases with a shift to higher binding energies as the coverage of Ca increases. Concerning the two surface components observed only in the intermediate phases, S4 has the same binding energy in the three phases, and S5 shifts to higher binding energies as the Ca coverage increases. The constant binding energies of S1, S3, and S4, and the continuous shifts of S2 and S5 indicate that the origin of each component is the same or quite similar in all phases. Below, we only investigate the geometric structures and discuss the origins of the surface components for the (3×2), (2×1), and (5×2) phases within the initial state effects, since the (3×2) and (2×1) are the two

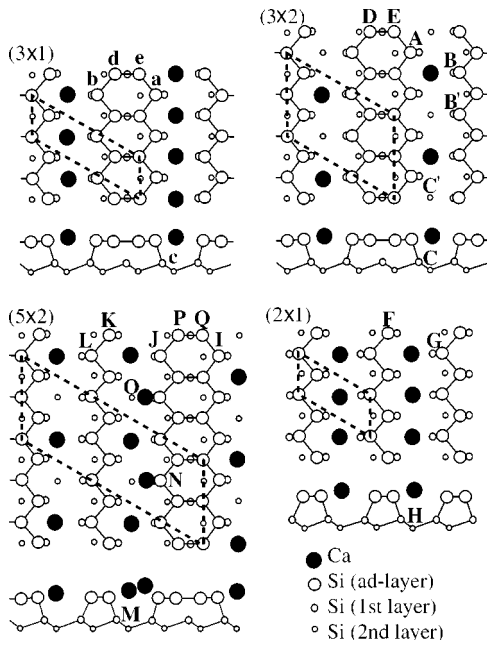


FIG. 5. Structural models for the Ca/Si(111) surfaces. The (3×1) phase with a Ca coverage of $1/3$ ML, the (3×2) phase with a Ca coverage of $1/6$ ML, the (5×2) phase with a coverage of 0.3 ML, and the (2×1) phase with a coverage of 0.5 ML. The model of the (3×1) is completely the same as that of the HCC model proposed for AM/Si(111)- (3×1) surfaces, and the geometric structure of Si atoms in the (3×2) phase is the same as the HCC structure. Filled circles are Ca atoms, and open circles are Si atoms. The dashed lines indicate the unit cells of each phase.

end phases of the series, and the (5×2) is a typical intermediate phase.

A. (3×2) and (2×1) phases

Based on *ab initio* calculations, the most energetically stable adsorption site of AEM atoms was reported to be the T_4 site (just above the second layer Si atoms) in the two structural models proposed for the so-called AEM/Si(111)- (3×1) surfaces, i.e., the HCC structures with AEM coverages of $1/3$ ML (Refs. 3,4) and $1/6$ ML.²³ Ca atoms were also reported to adsorb on the T_4 site in the Seiwatz model of the (2×1) phase.^{3,4} Comparing the experimental results and calculations performed on a $1/3$ ML Ca adsorbed Si(111)- (3×1) surface and on a 0.5 ML adsorbed (2×1) surface,³ the surface component observed on the lower binding energy side of the bulk component was assigned to originate from the Si atoms bonded directly to Ca atoms, i.e., the “*a*” and “*b*” Si atoms of the (3×1) phase and the “*F*” and “*G*” atoms of the (2×1) phase in Fig. 5. The surface component observed on the higher binding energy side of the bulk component was assigned to originate from the second layer Si atoms that are situated just below the Ca atoms, the “*c*” and “*H*” Si atoms in Fig. 5.³ However, since the number of surface components is different from that observed in the present study, i.e., only two surface components were observed for both the lowest and highest coverage phases in the previous study, we cannot just use these previous assign-

ments. Further, a structural model with a (3×1) periodicity and a Ca coverage of $1/3$ ML, was used to attribute the origins of the surface components of the lowest coverage phase in that study, while the periodicity of the basic structure is actually (3×2) as shown in the present study and the accurate Ca coverage of this phase was undetermined.

To investigate the geometric structure of the (3×2) phase, we first compare the present result with the previous Si $2p$ core-level studies performed on the $1/3$ ML AM’s adsorbed Si(111)- (3×1) surfaces.^{9,12,13,15,18} Due to the charge transfer from AM to Si, the two surface components, whose binding energies are lower than that of the bulk component, were attributed to originate from the surface Si atoms bonded directly to the adsorbate (the “*a*” and “*b*” Si atoms in Fig. 5).^{15,18} The difference in binding energy results from the different AM-Si bonding configuration, i.e., an “*a*” atom bonds to two AM atoms, whereas a “*b*” atom bonds to only one AM atom. In a theoretical calculation performed on the Na/Si(111)- (3×1) surface,¹⁸ the surface component with the lowest binding energy is assigned to originate from the “*b*” Si atoms, and the component with the second lowest binding energy is expected to result from the “*a*” atoms. Taking into account that different bonding configurations produce different surface components for the alkali metal adsorbed Si(111)- (3×1) surfaces, and that there are also two different Ca-Si bonding configurations in both the (3×1) and (3×2) phases as shown in Fig. 5, we regard the $S1$ and $S2$ components to originate from Si atoms that bond to Ca atoms and have different Ca-Si bonding configurations.

In order to discuss the origins of $S1$ and $S2$ in more details, we pay attention to the intensity ratio of the two components. This intensity ratio gives information about the number of corresponding Si atoms in the unit cell, which makes it possible to obtain more accurate information about the geometric structure of the (3×2) phase and to make more precise assignments of the origins of $S1$ and $S2$. Using a condition of $(h\nu, \theta_e) = (135 \text{ eV}, 60^\circ)$, the intensity ratios of $S1$ and $S2$ were approximately 7:1 for the (3×2) phase and 7:3 for the (2×1) phase. These intensity ratios were almost the same using a condition of $(h\nu, \theta_e) = (135 \text{ eV}, 0^\circ)$. However, as shown in Fig. 3, the intensity of $S1$ becomes smaller in the spectra obtained using other photon energies. Using photon energies of 125 and 145 eV, the intensity ratios of $S1$ and $S2$ were approximately 2:1 for the (3×2) phase, and 1:1 for the (2×1) phase. By comparing the intensity ratio obtained with $h\nu = 135 \text{ eV}$ and other photon energies, one notices that the intensity of $S1$ is enlarged at $h\nu = 135 \text{ eV}$ due to a diffraction effect. This means that the intensity ratio of the surface components obtained with $h\nu = 135 \text{ eV}$ does not correspond to the number ratio of Si atoms that produce $S1$ and $S2$. Since the intensity ratios obtained with other photon energies were identical, we conclude the intensity ratios of 2:1 and 1:1 to be the number ratios of Si atoms that produce $S1$ and $S2$ in the (3×2) phase and the (2×1) phase, respectively.

Even by modifying the Ca adsorption sites and by forming a (3×2) periodicity, a ratio of 2:1 cannot be achieved using a Ca coverage of $1/3$ ML, i.e., a coverage proposed in

the early studies.^{3,4} Since the accurate coverage of Ca was not measured in the early studies, and the 1/3 ML coverage was only based on the assumption that the coverage of Ca is the same as that of the AM/Si(111)-(3×1) surfaces, we have investigated the Ca coverage of the (3×2) phase by the Ca deposition time and the Ca 3*p* core-level spectra. In the present study, the (3×“2”) and (2×1) phases were obtained with a Ca deposition time ratio of 0.35:1, in the case of annealing the sample to 825 K following the room temperature adsorption. An annealing at 825 K hardly desorbs Ca atoms from the surface, and thus the deposition time is closely related to the Ca coverage supposing that the adsorption probability is constant for all coverages. The intensity ratio of the Ca 3*p* core-level spectra, normalized using the background intensities that are proportional to the photon flux, was 0.31:1 for the (3×“2”) and (2×1) phases. Based on these ratios and on the 0.5 ML Ca coverage of the (2×1) phase, we conclude that the Ca/Si(111)-(3×“2”) surface has the HCC structure with a Ca coverage of 1/6 ML. This conclusion indicates that the geometric structure of the Ca/Si(111)-(3×“2”) surface is the same as that of the Ba/Si(111)-(3×2) surface, and therefore supports the proposition²³ that the geometric structures of all AEM's adsorbed Si(111)-(3×“2”) surfaces are universal.

By using the 1/6 ML model, we consider the origins of *S1* and *S2* of the (3×“2”) phase. As shown in the 1/6 ML (3×2) model in Fig. 5, the number ratio of the “*A*” and “*B*” Si atoms is 2:1 in the unit cell. This ratio fits with the ratio of *S1* and *S2*. In the case of attributing *S1* and *S2* to the “*A*” and “*B*” Si atoms, respectively, the assignment becomes different from that done for the AM/Si(111)-(3×1) surfaces. That is, the surface component with the lowest binding energy is attributed to originate from the “*b*” Si atoms in the case of AM that correspond to the “*B*” atoms of the (3×2) phase in Fig. 5. Taking the difference in adsorbate into account, this conflict can be explained by the symmetry of the surface structure and the difference in the number of valence electrons. The dangling bonds of the “*b*” and “*B*” Si atoms face the adsorbates, whereas the dangling bonds of the “*a*” and “*A*” atoms should change their direction to interact with the *s* orbitals of the adsorbates. This means that in the case of an AM/Si(111)-(3×1) surface, an *s* orbital of monovalent adsorbate energetically prefers to interact with a dangling bond of the *b* Si atom. The preferable interaction indicates that the amount of charge transfer from AM atoms to the *b* Si atoms should be larger than that to the *a* atoms, and that the energy shift of the surface component produced by the *b* Si atoms is larger than the component produced by the *a* atoms. On the other hand, the *s* orbitals of a divalent AEM atom would energetically prefer to interact with two dangling bonds rather than only one dangling bond. By assuming that the interaction between a Ca atom and two symmetric dangling bonds is energetically preferable though the dangling bonds have to change their direction, the amount of charge transfer from the Ca atoms to the *A* Si atoms becomes larger than that to the *B* atoms of the (3×2) phase. Therefore, we conclude that the origins of *S1* and *S2* observed in the (3×“2”) phase are the *A* and *B* Si atoms, respectively.

Regarding the (2×1) phase, there are also two different Ca-Si bonding configurations in the Seiwatz model, i.e., each *F* Si atom bonds to two Ca atoms and each *G* atom bonds to one Ca atom as shown in Fig. 5. The good agreement in the number ratio of the *F* and *G* atoms and the intensity ratio of *S1* and *S2* (1:1) supports that the geometric structure of the (2×1) phase is the Seiwatz structure with a Ca coverage of 0.5 ML. By using the same discussion as for the (3×“2”) phase, the *s* orbitals of Ca atoms should energetically prefer to interact with the dangling bonds of the *F* Si atoms. This means that the origins of *S1* and *S2* of the (2×1) phase might be the *F* and *G* Si atoms, respectively. The distance between Ca atoms and the *G* Si atoms is longer than the distance between Ca atoms and the *B* atoms, and thus the interaction between Ca and *G* atoms should be weaker than that between Ca and *B* atoms. Since a weaker interaction suggests a smaller amount of charge transfer, we conclude that the origin of *S2* of the (2×1) phase is the *G* Si atoms. Further, the smaller amount of charge transfer explains well the energy shift of *S2* observed in Figs. 3 and 4.

As in the case of the *G* and *B* atoms, the distance between Ca atoms and the *F* atoms is larger than the distance between Ca atoms and the *A* atoms. The weaker interaction between Ca atoms and the *F* atoms should produce an energy shift of *S1* to a higher binding energy. On the other hand, the numbers of Ca-Si bonds of the *A* and *F* atoms are different. That is, the *A* Si atoms bond to only one Ca atom, while the *F* Si atoms bond to two Ca atoms. A larger number of Ca-Si bonds suggests a larger amount of charge transferred into the *F* atoms, and therefore a shift of *S1* to a lower binding energy. By assuming that the effect of the larger number of bonding orbitals is canceled by the weaker interaction, we attribute the origin of *S1* in the (2×1) phase to be the *F* atoms.

The third surface component observed in the (3×“2”) and (2×1) phases (*S3*) was reported to originate from the Si atoms that form the honeycomb and are not bonded to the adsorbate for the AM adsorbed Si(111)-(3×1) surface, i.e., the *d* and *e* Si atoms in Fig. 5.^{15,18} On the other hand, *S3* is stated to originate from the second layer Si atoms situated just below the adsorbate in a theoretical calculation done for the 1/3 ML Ca adsorbed Si(111)-(3×1) surface (the *c* Si atoms).³ In the present study, *S3* is observed in all phases at the same binding energy. The constant binding energy indicates that the origin of *S3* should be basically the same in all phases. Since there is no honeycomb in the (2×1) phase, the second layer Si atoms situated just below the adsorbate are more probable as the origin of *S3*. However, the FWHM of *S3* is larger than the FWHM's of *S1* and *S2* in the (3×“2”) phase, while the FWHM's of the three components are almost the same in the (2×1) phase. In the (3×“2”) phase, the FWHM of *S3* is 290 meV and those of *S1* and *S2* are 268 and 272 meV, respectively. The larger FWHM suggests the possibility of more than one origin for the *S3* of the (3×“2”) phase. Therefore, since it is hard to exclude the possibility of other origins for the (3×“2”) phase, we attribute *S3* to the *C*, *D*, and *E* atoms for the (3×“2”) phase, and to the *H* atoms for the (2×1) phase.

Here, we would like to mention briefly about the B and C atoms of the $1/6$ ML (3×2) model, which have dangling bonds. The presence of dangling bonds indicates that the environments of the B and C atoms are different from the bulk Si atoms, and thus can be the origin of one of the surface components. However, taking into account that there is no Si atoms with dangling bonds in the (2×1) phase and that the origin of each surface component is the same or quite similar in all phases, these atoms cannot be the origin of a surface component observed in the present study. Within the initial state effects, this result can be explained by the charge states of the B and C atoms. That is, if there is no charge transfer from or into the B and C atoms, the charge states of these atoms are the same as the charge states of bulk Si atoms, and therefore the binding energies of the surface components, which originate from these atoms, should be the same as the binding energy of the bulk component.

B. (5×2) phase

In order to investigate the geometric structure of the (5×2) phase, we consider the origins of $S4$ and $S5$. Of the $S4$ and $S5$ components, $S4$ was also reported in the Si $2p$ core-level study of divalent rare-earth metals (Sm and Yb) adsorbed Si(111)-(5×1) surfaces, which were also proposed to be formed by a combination of the rare-earth metals induced (3×2) and (2×1) phases.^{25,26} In this previous study, $S4$ is attributed to originate from the dimers of the first layer Si atoms. Here, we notice that the structural models of the (3×2) and (2×1) phases used in this previous study are different from the HCC and Seiwatz models, i.e., Sm and Yb atoms were proposed to be adsorbed in the bridge sites of an ideal Si(111)-(1×1) surface. Thus, we cannot use the assignment of $S4$ derived for rare-earth metals adsorbed surfaces.

Although the observation of the (5×2) LEED pattern suggests that this phase might be basically formed by the combination of the (3×2) and (2×1) phases, the presence of the $S4$ and the $S5$ components indicates a more complex situation. Taking these conditions into account, we propose that the geometric structure of the Si atoms follows the HCC and Seiwatz models, while not all Ca atoms are adsorbed on the T_4 sites as suggested in the literature. The Ca coverage of the (5×2) phase was reported to be 0.4 ML in the previous studies.^{3,4} This coverage determination was based on the fact that only a (5×1) periodicity and no trace of the $\times 2$ periodicity was observed in these studies. That is, the adsorption of one Ca atom in the (5×1) unit cell leads to a coverage of 0.2 ML that is lower than their estimated coverage for the (3×2) phase, and the adsorption of three Ca atoms in the (5×1) unit cell leads to a coverage of 0.6 ML that is higher than the coverage of the (2×1) phase. However, there is no experimental evidence about the coverage in the previous study, and the periodicity of the basic structure is obtained to be (5×2) in the present study. To investigate the Ca coverage of the (5×2) phase, we compare the Ca deposition time and the Ca $3p$ core-level spectra with those of the (3×2) phase. The Ca deposition time to obtain the (5×2) phase was 1.86 times longer

than that to obtain the (3×2) phase, and the intensity of the Ca $3p$ core-level was 1.74 times higher than that of the (3×2) phase. Since the coverage of the (3×2) phase is $1/6$ ML, these ratios indicate that the Ca coverage of the (5×2) phase is 0.3 ML. Therefore, we conclude that the Ca coverage of the (5×2) phase is 0.3 ML, and the coverage reported in the previous studies^{3,4} was overestimated. The 0.3 ML Ca coverage supports that the (5×2) phase is basically formed by the combination of the (3×2) and (2×1) phases.

Since the energy shift of $S4$ is larger than that of $S1$ and $S2$, a possible assignment of its origin is the Si atoms with a larger amount of charge transferred from Ca. Such large charge can be transferred in the case of a larger number of Ca-Si bonding orbitals per Si atom and/or a stronger interaction between the Ca s orbital and the Si dangling bond, which is formed by a shorter Ca-Si bond length. As shown in Fig. 4, the intensity of $S4$ is smaller than those of the $S1$ and $S2$ components. By considering that $S1$ and $S2$ should originate from Si atoms that are situated on the T_4 site and bond to Ca, the small intensity of $S4$ suggests that among the three Ca atoms in the unit cell, one of them bonds to a Si atom with a Ca-Si bond length shorter than the other two Ca atoms. Based on these suggestions, we propose a structural model of the (5×2) phase that is shown in Fig. 5. According to this structural model, we attribute the origin of $S4$ to the N Si atoms, which have the shortest Ca-Si bond length.

The I and J Si atoms have the same coordination as the A and B atoms of the (3×2) phase, and the L atoms have the same coordination as the G atoms of the (2×1) phase. The equivalencies in coordination indicate that the I atoms produce $S1$, and the J and L atoms produce $S2$. On the other hand, the coordination of the K atoms is slightly different from that of the F atoms of the (2×1) phase, i.e., only one Ca atom bonds to the K atoms whereas two Ca atoms are situated near the F atoms. The lower number of surrounding Ca atoms per Si atom suggests a lower amount of charge transfer into these Si atoms. Thus, by assuming that the amount of charge transfer into the K atoms is almost the same as the amount transferred into the J and L atoms, the K atoms might also contribute to $S2$. In this case, the intensity ratio of $S1$, $S2$, and $S4$ should be the same as the ratio of $I:(J+K+L):N$ in the (5×2) unit cell, which is 2:5:1. This ratio is in good agreement with the intensity ratio of $S1$, $S2$, and $S4$ obtained experimentally, which varied from 2:4:1 to 3:6:1 depending on the experimental condition for the (5×2) phase. Therefore, we attribute $S1$ and $S2$ of the (5×2) phase to the I atoms, and to the combination of the J , K , and L atoms, respectively.

Finally, we discuss the origin of $S5$. $S5$, which is observed only in the intermediate phases in similarity with $S4$, shows the highest binding energy. In the (3×2) phase, the Si $2p$ component that has a higher binding energy than the bulk component originates from the C atoms and/or the D and E atoms. In the (2×1) phase, the higher binding energy component originates from the H atoms. This means that the second layer Si atoms situated just below the Ca atoms and the Si atoms that form the honeycomb but are not bonded to

Ca atoms are positively charged in the (3×2) and (2×1) phases. The large amount of charge transferred into the N atoms can change the charge states of the Si atoms that form the honeycomb but are not bonded to Ca atoms, and the slightly different Ca adsorption site can also change the charge states of the second layer Si atoms. Thus, although there is no strong evidence, we propose the origin of $S5$ to be the O atoms and/or the P and Q atoms in Fig. 5.

V. CONCLUSION

In conclusion, we have studied the surface structures of different Ca/Si(111) surfaces by LEED and high-resolution core-level photoelectron spectroscopy. (3×2) , (5×2) , (7×2) , (9×2) , and (2×1) phases were observed in LEED at different Ca coverages. In the Si $2p$ core-level spectra, three surface components ($S1$, $S2$, and $S3$) were observed in both the (3×2) and (2×1) phases. These three surface components are also observed in the three intermediate phases together with two other components ($S4$ and $S5$). The binding energies of $S1$ and $S3$ are the same in all phases, and the binding energy of $S2$ shifts to higher binding energies as the Ca coverage increases. $S4$ is observed at the same binding energy in the three intermediate phases, and $S5$ shows a continuous shift toward higher bind-

ing energies as the Ca coverage increases. These results indicate that the origin of each component is the same in each phase. By considering the energy shift and intensity of each surface component, we conclude that the structures of the (3×2) and (2×1) phases are given by the HCC model with a Ca coverage of $1/6$ ML and the Seiwatz model with a coverage of 0.5 ML, respectively. Regarding the (5×2) phase, the observation of the $\times 2$ periodicity in LEED, a Ca coverage of 0.3 ML, and the presences of $S4$ and $S5$ in the core-level studies indicate that the geometric structure of the Si atoms of this phase is basically formed by a combination of the two end phases, while not all Ca atoms are adsorbed on the T_4 sites as suggested in the literature. Taking the energy shift and the intensity of $S4$ into account, we have proposed a structural model of the Ca/Si(111)- (5×2) surface.

ACKNOWLEDGMENTS

Experimental support from Dr. T. Balasubramanian and the MAX-lab staff, and suggestions on the sample preparation from Dr. T. Sekiguchi are gratefully acknowledged. This work was financially supported by the Swedish Research Council and the Carl Trygger Foundation (K.S.).

*Electronic address: sakamoto@surface.phys.tohoku.ac.jp

¹P. Segovia, D. Purdie, M. Hengsberger, and Y. Baer, *Nature (London)* **402**, 504 (1999).

²H.W. Yeom, S. Takeda, E. Rotenberg, I. Matsuda, K. Horikoshi, J. Schaefer, C.M. Lee, S.D. Kevan, T. Ohta, T. Nagao, and S. Hasegawa, *Phys. Rev. Lett.* **82**, 4898 (1999).

³A.A. Baski, S.C. Erwin, M.S. Turner, K.M. Jones, J.W. Dickinson, and J.A. Carlisle, *Surf. Sci.* **476**, 22 (2001).

⁴T. Sekiguchi, F. Shimokoshi, T. Nagao, and S. Hasegawa, *Surf. Sci.* **493**, 148 (2001).

⁵W.C. Fan and A. Ignatiev, *Phys. Rev. B* **41**, 3592 (1990).

⁶J. Quinn and F. Jona, *Surf. Sci.* **249**, L307 (1991).

⁷K.J. Wan, X.F. Lin, and J. Nogami, *Phys. Rev. B* **46**, 13 635 (1992); **47**, 13 700 (1993).

⁸D. Jeon, T. Hashizume, T. Sakurai, and R.F. Willis, *Phys. Rev. Lett.* **69**, 1419 (1992).

⁹J.J. Paggel, G. Neuhold, H. Haak, and K. Horn, *Phys. Rev. B* **52**, 5813 (1995).

¹⁰A.A. Saranin, A.V. Zotov, V.G. Lifshits, M. Katayama, and K. Oura, *Surf. Sci.* **426**, 298 (1999).

¹¹O. Kubo, A.A. Saranin, A.V. Zotov, J.-T. Ryu, H. Tani, T. Harada, M. Katayama, V.G. Lifshits, and K. Oura, *Surf. Sci.* **415**, L971 (1998).

¹²T. Okuda, H. Daimon, S. Suga, Y. Tezuka, and S. Ino, *Appl. Surf. Sci.* **121/122**, 89 (1997).

¹³H.H. Weitering, X. Shi, and S.C. Erwin, *Phys. Rev. B* **54**, 10 585 (1996).

¹⁴K. Sakamoto, H. Ashima, H.M. Zhang, and R.I.G. Uhrberg, *Phys. Rev. B* **65**, 045305 (2002).

¹⁵K. Sakamoto, H.M. Zhang, and R.I.G. Uhrberg, *Surf. Rev. Lett.* **9**, 1235 (2002).

¹⁶S.C. Erwin and H.H. Weitering, *Phys. Rev. Lett.* **81**, 2296 (1998).

¹⁷L. Lottermoser, E. Landemark, D.-M. Smilgies, M. Nielsen, R. Feidenhans'I, G. Falkenberg, R.L. Johnson, M. Gierer, A.P. Seitsonen, H. Kleine, H. Bludau, H. Over, S.K. Kim, and F. Jona, *Phys. Rev. Lett.* **80**, 3980 (1998).

¹⁸M.-H. Kang, J.-H. Kang, and S. Jeong, *Phys. Rev. B* **58**, R13 359 (1998).

¹⁹T. Okuda, K. Sakamoto, H. Nishimoto, H. Daimon, S. Suga, T. Kinoshita, and A. Kakizaki, *Phys. Rev. B* **55**, 6762 (1997).

²⁰K. Sakamoto, T. Okuda, H. Nishimoto, H. Daimon, S. Suga, T. Kinoshita, and A. Kakizaki, *Phys. Rev. B* **50**, 1725 (1994).

²¹K.S. An, R.J. Park, J.S. Kim, C.Y. Park, C.Y. Kim, J.W. Chung, T. Abukawa, S. Kono, T. Kinoshita, A. Kakizaki, and T. Ishii, *Surf. Sci.* **337**, L789 (1995).

²²T. Okuda, H. Ashima, H. Takeda, K.S. An, A. Harasawa, and T. Kinoshita, *Phys. Rev. B* **64**, 165312 (2001).

²³G. Lee, S. Hong, H. Kim, D. Shin, J.-Y. Koo, H.-I. Lee, and D.W. Moon, *Phys. Rev. Lett.* **87**, 056104 (2001).

²⁴H.H. Weitering, *Surf. Sci.* **355**, L271 (1996).

²⁵C. Wigren, J.N. Andersen, R. Nyholm, M. Göthelid, M. Hammar, C. Törnevik, and U.O. Karlsson, *Phys. Rev. B* **48**, 11 014 (1993).

²⁶C. Wigren, J.N. Andersen, R. Nyholm, U.O. Karlsson, J. Nogami, A.A. Baski, and C.F. Quate *Phys. Rev. B* **47**, 9663 (1993).